Eurasian Journal of Physics and Functional Materials

2020, 4(4), 309-318

Study of the influence of the phase composition and crystal structure of Fe_xNi_{100-x} nanostructures on the efficiency of using lithium-ion batteries as anode materials

D.B. Borgekov[1,2], N.A. Hlebnikov[3], D.I. Shlimas[1,2], A.L. Kozlovskiy*[,2,4]

[1]Engineering Profile Laboratory, L.N. Gumilyov Eurasian National University, Nur-Sultan, Kazakhstan

[2]Laboratory of Solid State Physics, The Institute of Nuclear Physics, Almaty, Kazakhstan

[3]Department of Intelligent Information Technologies, Ural Federal University, Yekaterinburg, Russia

[4]Kazakh-Russian International University, Aktobe, Kazakhstan

E-mail: kozlovskiy.a@inp.kz

DOI: **10.29317/ejpfm.2020040404**
Received: 10.10.2020 - after revision

The results of the efficiency of using Fe_xNi_{100-x} nanotubes as anode materials for lithium-ion batteries have been obtained. In the course of research, it was found that an increase in the concentration of nickel in the structure to 40 and 60 at.% leads to a sharp increase in the resource number of cycles by more than two times in comparison with iron nanotubes. Such a difference in the resource lifetime is due to the higher stability of Fe_xNi_{100-x} nanotubes with a nickel concentration of more than 40 at.% to destruction, as well as resistance to oxidation.

Keywords: nanotubes, structural ordering, degradation, anode materials, Li-ION batteries.

Introduction

In the modern world, one of the most promising nanomaterials for microelectronics and power supplies are cylindrical nanostructures based on iron-nickel,

which have a large number of free charge carriers, a developed active surface, high conductivity and magnetic characteristics [1-5]. Nanostructures based on $Fe_x Ni_{100-x}$ possess unique physicochemical properties when the synthesis conditions or chemical composition change, which allows them to be one of the versatile materials with wide potential applications. In connection with the foregoing, it is of particular interest to study the effect of irradiation with protons and low-energy ions on the structural and heat-conducting properties of ceramic materials, since the problem of the radiation resistance of nitride ceramics has not yet been fully resolved.

One of the most promising applications of nanostructures in modern microelectronics and power engineering is the creation on their basis of microaccumulators or energy storage devices, which will have greater competitiveness with the existing analogs based on silicon and carbon [6-8]. At the same time, the use of cheap nanomaterials based on iron/nickel compounds will reduce the risk of pollution and environmental poisoning of wildlife when disposing of batteries containing lead. The use of cylindrical hollow nanostructures can significantly increase the specific surface area due to the outer and inner surfaces of the nanotube wall. This circumstance will significantly increase the rate of lithiation and battery charging [9-13].

Experimental part

Synthesis of microtubules was carried out using the electrochemical synthesis method using a two-electrode cell, where copper plates were used as the cathode and anode. The composition of the electrolyte solution for obtaining iron and iron-nickel microstructures: Iron (II) sulphate heptahydrate ($FeSO_4 \times 7H_2O$), Nickel (II) sulphate heptahydrate ($NiSO_4 \times 7H_2O$) in the required molar ratio, boric acid (H_3BO_3) and ascorbic acid ($C_6H_8O_6$). All dissolved components were poured into one flask, and ascorbic acid was added to control the pH level. All used chemical reagents were of analytical grade (the content of the main component was higher than 98%) or chemically pure (the content of the main component was more than 99%). All components were purchased from Sigma Aldrich.

The control over the deposition processes was carried out using the chronoamperogram method, which allows high-precision control of the deposition and formation of nanostructures in the pores of template matrices. Polymer films based on polyethylene terephthalate, obtained using ion-track technology, were used as template matrices. The first stage consists in irradiation of films with heavy ions Kr15+ with energy of 1.75 MeV/nucleon and beam density of 4×10^7 ion/cm^2, irradiation angle of 90° relative to film surface. Irradiation under specified conditions makes it possible to obtain latent tracks in polymer film, direction of which coincides with direction of irradiation. The second stage consists in chemical etching of latent tracks to a given geometry. A 2.2 M sodium hydroxide solution was used as an etchant solution, etching was carried out at a temperature of 85°C, the etching time for obtaining diameters of 380-400 nm was

5 minutes. Figure 1 shows a schematic representation of the process of obtaining microstructures using the chronoamperometry method.

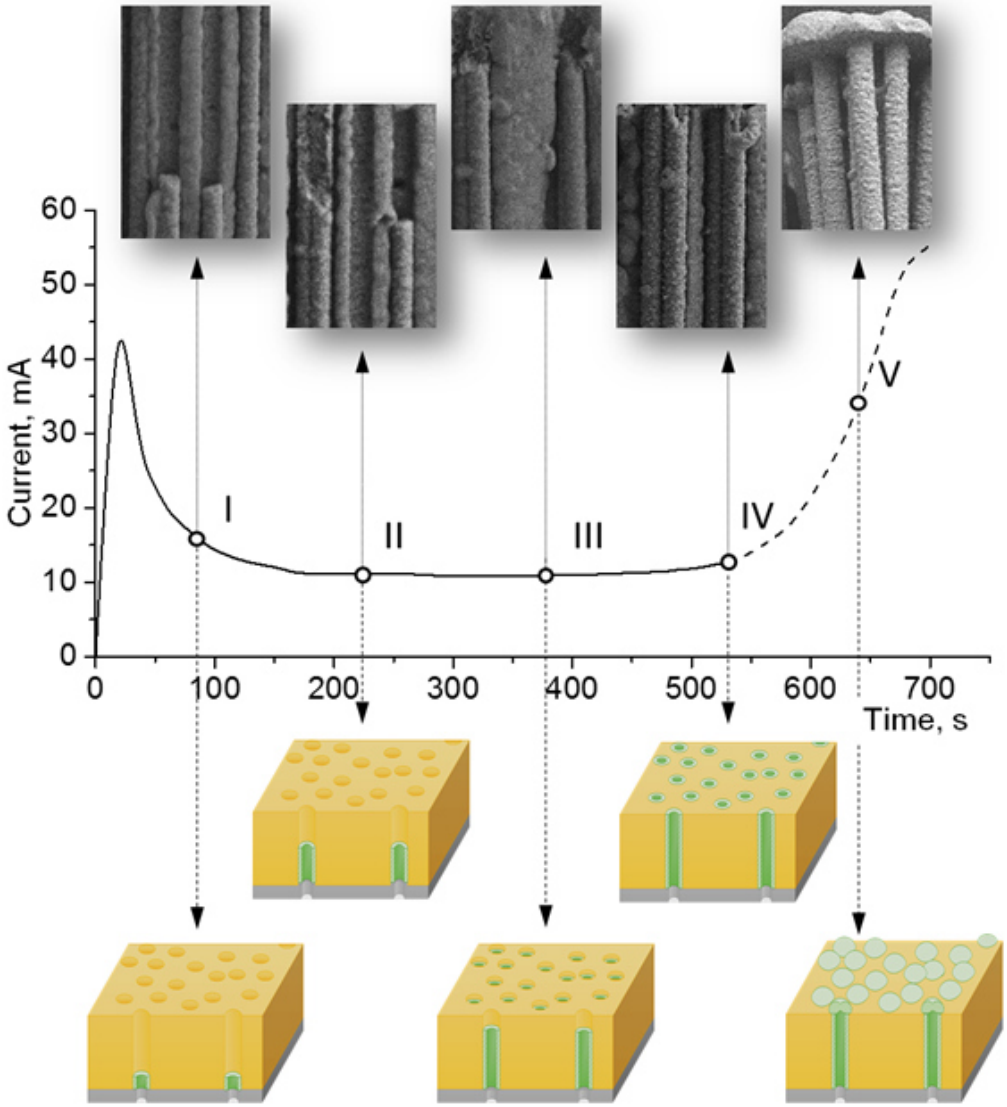

Figure 1. Chronoamperogram of the deposition process with a schematic representation of the stages of formation of microtubes with a length of: 3 μm (I); 6 μm (II); 9 μm (III); 12 μm (IV), and also after the formation of "caps" (V).

Electrochemical deposition of microstructures was carried out at an applied potentials difference of 1.75 V, the choice of which is based on the knowledge of the potentials of the reduction of iron and nickel ions from electrolyte solutions. To obtain structures with a given elemental composition and crystal structure, the ratio of metal salts was varied in the preparation of electrolyte solutions. The change in salt concentration resulted in five microstructure compositions in which the elemental nickel content ranged from 0 to 81 atom %. Component content was determined using the energy dispersion analysis method by measuring spectra from various sections of microtubes, as well as removing element distribution maps to estimate isotropy of component distribution in the microtubes structure. Figure 2 shows typical data of scanning electron microscopy and mapping results of the studied microstructures.

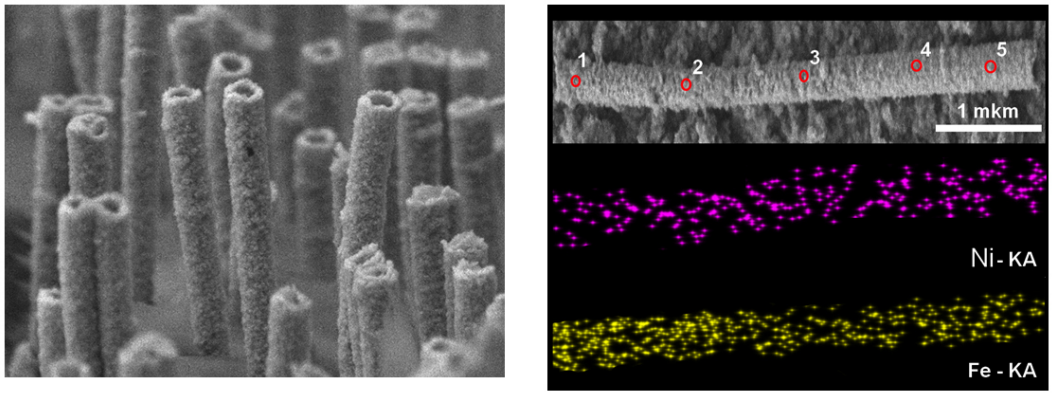

a) b)

Figure 2. a) SEM images of synthesized microtubes; b) Example of elemental analysis measurement results: 1 – $Fe_{59,45}Ni_{40,55}$, 2 – $Fe_{59,37}Ni_{40,63}$, 3 – $Fe_{58,95}Ni_{41,05}$, 4 – $Fe_{59,58}Ni_{40,42}$, 5 – $Fe_{58,79}Ni_{41,21}$.

The study of the phase composition of the synthesized samples was carried out using the method of X-ray phase analysis. Analysis of the obtained diffraction patterns showed the following: at an iron concentration of 80 and 60 atom. %, the bcc phase predominates in the structure of microtubes; in this case, with an increase in the iron concentration, an increase in the crystal lattice parameter is observed from 2.8823 Å for $Fe_{80}Ni_{20}$ to 2.8894 Å for $Fe_{60}Ni_{40}$. At the same time, for the $Fe_{40}Ni_{60}$ sample, the most intense peak is observed, characteristic of connecting FeNi3 with Miller indices (111) with a cell parameter of 3.5939 Å . For $Fe_{20}Ni_{80}$ sample, the nickel phase hcc with elemental cell parameter 3.5732 A prevails in the crystal structure. A detailed study of changes in structural parameters and phase composition in iron-nickel micro and nanostructures was previously investigated by us in works [14-16].

The following types of nanostructures were selected as objects of study for testing nanostructures as anode materials for lithium-ion batteries and creating a new class of batteries for microelectronics based on them, the characteristics of which are presented in Table 1.

Table 1.
Characterization of samples.

No	Sample name	Structure type	Atomic ratio, %
1	$Fe_{20}Ni_{80}$	FeNi-FCC, a=3.5732 Å	Fe – 19 at. %, Ni – 81 at. %
2	$Fe_{40}Ni_{60}$	FeNi-FCC, a=3.5939 Å	Fe – 38 at. %, Ni – 62 at. %
3	$Fe_{60}Ni_{40}$	Fe-BCC, a=2.8894 Å	Fe – 61 at. %, Ni – 39 at. %
4	$Fe_{80}Ni_{20}$	Fe-BCC, a=2.8823 Å	Fe – 79 at.%, Ni – 21 at. %
5	Fe_{100}	Fe-BCC, a=2.8751 Å	Fe - 100 at.%
Geometry of nanostructures		Nanotubes with a height of 12 μm, an outer diameter of 400 nm, and a wall thickness of 120-150 nm	

The composition of the electrolyte solution for obtaining iron and iron-nickel nanostructures: 7-aqueous sulfates of iron and nickel – $FeSO_4 4 \times 7H_2O$, $NiSO_4 \times 7H_2O$ in the required molar ratio, boric acid – H_3BO_3 and ascorbic

acid $C_6H_8O_6$. All dissolved components were poured into one flask, and ascorbic acid was added to control the pH level. All used chemical reagents were of analytical grade (the content of the main component was higher than 98%) or chemically pure (the content of the main component was more than 99%).

Electrochemical tests of the use of nanostructures as cathode materials for lithium-ion batteries were carried out in two-electrode CR20 32 cells on a CT-3008W-5V charge-discharge test bench. The electrolyte solution was a mixture of 1 M $LiPF_6$ ethylene carbonate/propylene carbonate/diethyl carbonate/ethyl methyl carbonate/propyl acetate. Cycling of the anodes was carried out in the range from 10 mV to 3 V, in the mode of limiting the charging capacity of 1000 mA·h/g. In the anode cycle, the limitation was the achievement of a voltage of –2 V [17, 18].

Investigation of the degree of degradation of nanostructures after cycles of test life was carried out using solution electron microscopy performed on a JEOL-7500F microscope at an accelerating voltage of 5.0 kV and a SEI scanning mode.

Results and discussion

Figures 1 show the results of life tests of the investigated nanostructures in the mode of testing the lifetime of cathode materials during life tests in the case of a charging capacity of 1000 mA · h/g.

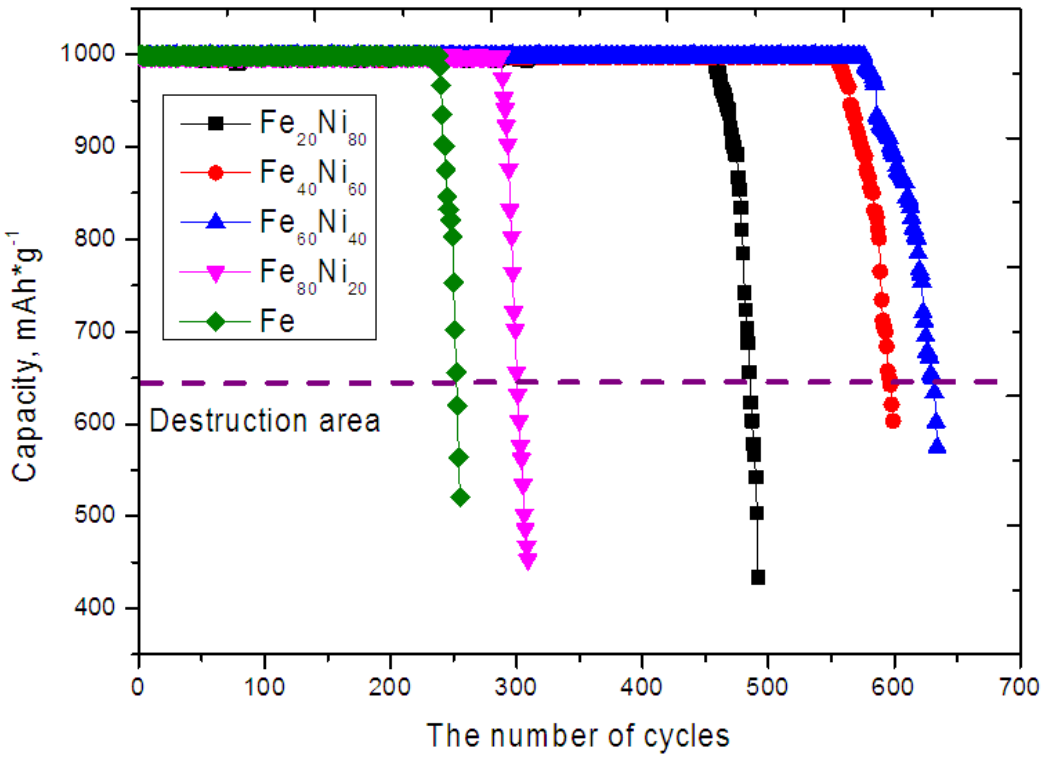

Figure 3. Graphs of the dependence of the specific discharge capacity on the number of cycles in the charging capacity mode of 1000 mA · h/g.

According to the data obtained, for all studied nanotubes, the change in the

capacity value with an increase in the life test cycles has two different sections. The first section is characterized by the preservation of the capacity value within the range of 995-1000 mA · h/g, which indicates the preservation of the operability of the anode material during lithiation, which is accompanied by the processes of oxidation and introduction of lithium into the structure, followed by charge transfer. The second section is characterized by a sharp drop in the capacity value, which means degradation of the anode material and a decrease in the efficiency of charge storage. Figure 2 shows data on the effect of the concentration of nickel in the structure of nanotubes on the number of cycles before the onset of the stage of material destruction.

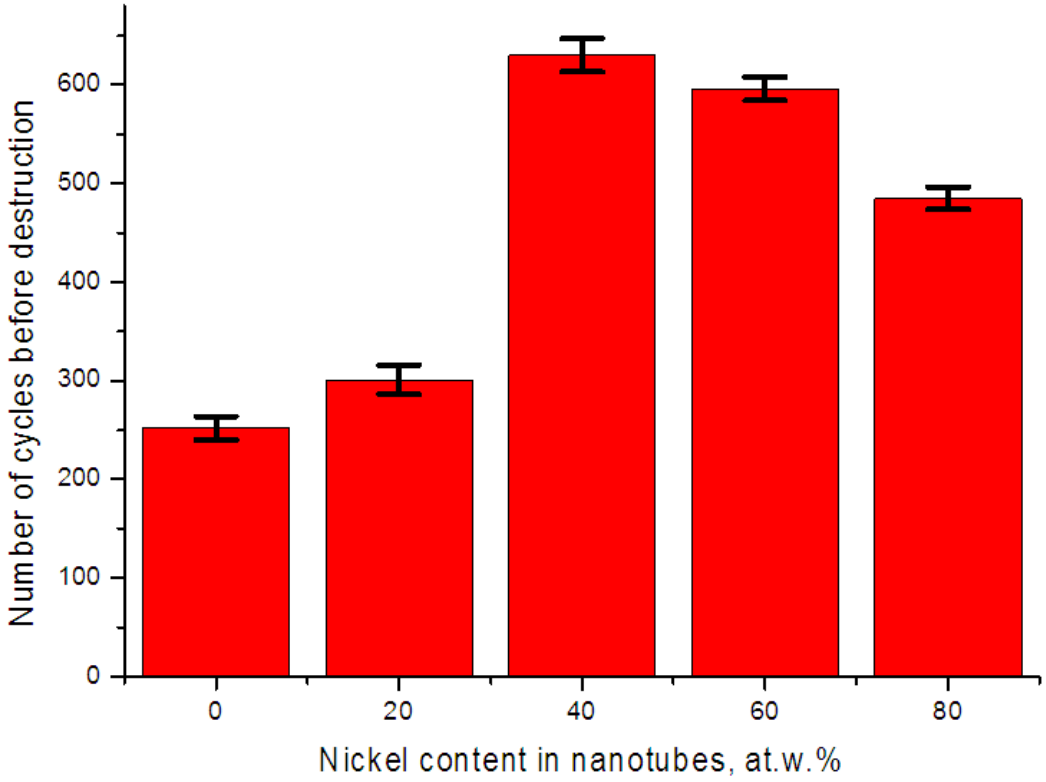

Figure 4. Diagram of the efficiency of the resource lifetime of $Fe_x Ni_{100-x}$ nanotubes.

The smallest number of test cycles before the stage of a sharp decrease in the capacity of the anode material is observed for Fe and $Fe_{80}Ni_{20}$ nanotubes, while an increase in the nickel concentration in the structure to 40 and 60 at.% leads to a sharp increase in the resource number of cycles by more than two times in comparison with iron nanotubes. This difference in the resource lifetime is due to the higher stability of $Fe_x Ni_{100-x}$ nanotubes with a nickel concentration of more than 40 at.% To destruction, as well as resistance to oxidation. Also for $Fe_x Ni_{100-x}$ nanotubes with an atomic nickel content of more than 60 at.%, the formation of the FeNi phase with a face-centered crystal lattice is characteristic, which also affects the lithiation processes.

A decrease in the capacity value, as a rule, occurs as a result of partial or complete destruction of the anode material, as well as the formation of a large number of amorphous and oxide inclusions in the structure of the material, thereby deforming it. Figure 3 shows typical SEM images of nanotubes before

and after life tests.

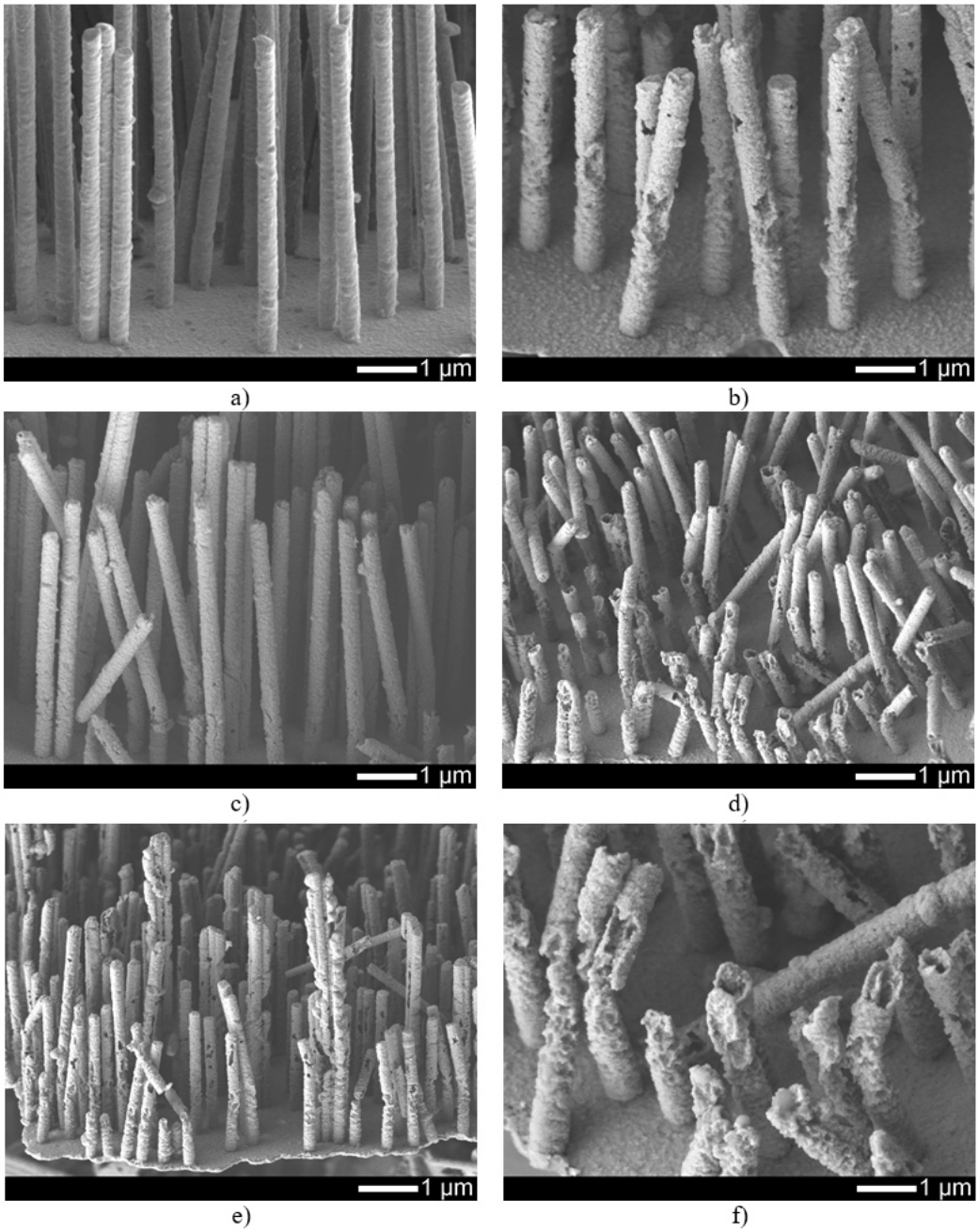

Figure 5. SEM images of nanotubes before and after life tests: a) $Fe_{20}Ni_{80}$ nanotubes prior to testing; b) $Fe_{20}Ni_{80}$ nanotubes after life tests; c) $Fe_{40}Ni_{60}$ nanotubes after life tests; d) $Fe_{60}Ni_{40}$ nanotubes after life tests; e) $Fe_{80}Ni_{20}$ nanotubes after life tests; f) Fe nanotubes after life tests.

As can be seen from the presented data, the greatest degree of structural destruction of nanotubes in the course of resource tests is observed for iron nanotubes, while nanotubes in which the nickel content is from 80 to 40 at.% the degree of destruction is much less. The main mechanisms of the destruction of nanotubes in the course of life tests are associated with the processes of oxidation and destruction as a result of the formation of pitting corrosion and amorphization of the structure. In this case, in structures with a high iron content, corrosion processes are more intensive due to the formation of oxide phases FeO, Fe_2O_3, Fe_3O_4, with a variable valence of Fe ions, which leads to destabilization

of the phase composition of nanotubes. In nanotubes with a high nickel content, which are characterized by a face-centered FeNi phase, oxidation occurs due to the formation of oxide spinels of the $NiFe_2O_4$ type, which are more resistant to degradation than simple iron oxides [19-21].

Studies of the influence of the charge/discharge rate were carried out in order to determine the possibility of using these nanostructures in batteries with fast charging, as well as to maintain their resistance to various charge/discharge rates. The value of the charge/discharge rate was C=250 mA/g, the rate was varied in the range from 1C to 10C and a return to the charge rate of 5C and 1C. The number of cycles at the same charge/discharge rate was 10 cycles.

Figure 4 shows the data on changes in the effect of the charge/discharge rate on the preservation of the specific capacity of the anode material for the studied nanotubes.

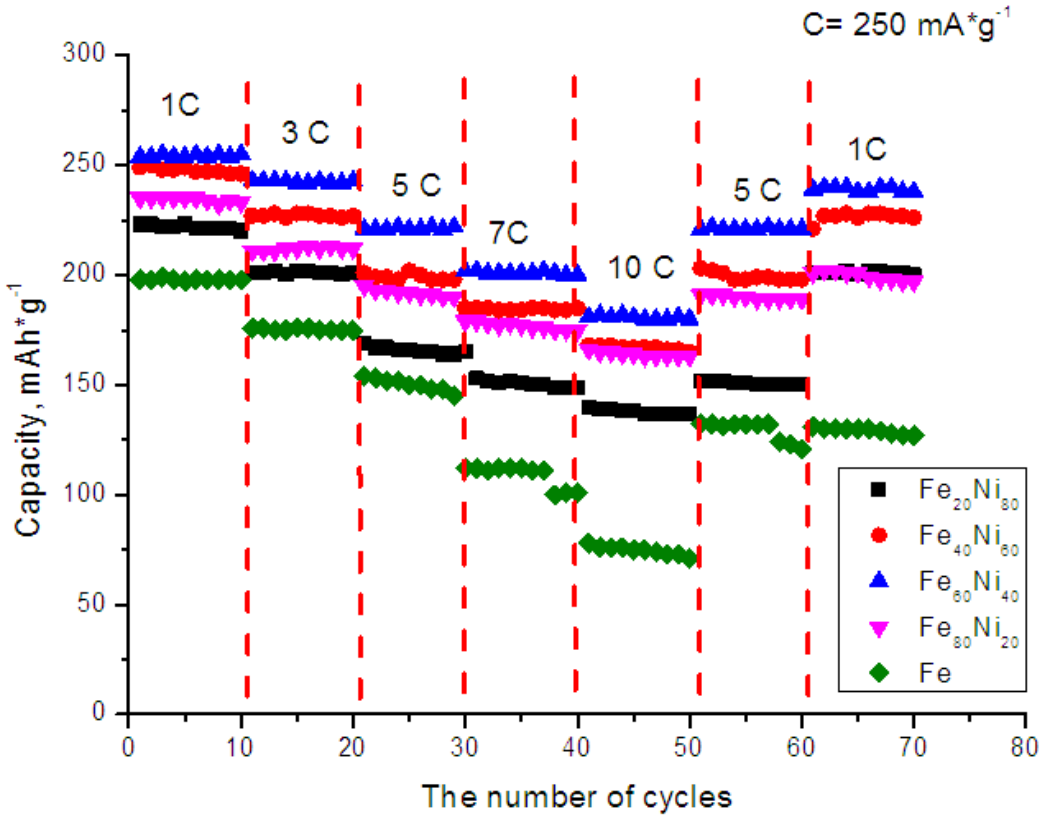

Figure 6. Data of changes of specific capacity value depending on battery charge/discharge rate.

As can be seen from the presented data, in the case when the charge/discharge rate is 1C, for $Fe_{60}Ni_{40}$ nanotubes the specific capacity is 248-250 mAh/g, while for other nanostructures this value decreases by 5-20%, depending on phase composition of nanotubes. A 20% decrease in the specific capacity for iron nanotubes is due to the low rate of lithiation processes, as well as to the oxidation of nanotubes with the formation of oxide impurities. An increase in the charge/discharge rate up to 3C and 5C leads to a decrease in the value of the specific capacity, but at the same time the value is preserved during all charge/discharge cycles. However, for iron nanotubes, an increase in the

charge/discharge rate to 7C and 10C leads to a deterioration in maintaining the specific capacity for a long time. A decrease in the charge/discharge rate led to the return of the specific capacity to the initial values for $Fe_{60}Ni_{40}$ and $Fe_{40}Ni_{60}$ nanotubes, which indicates the stability of all nanostructures to fast charging processes. For the rest of the nanotubes, a decrease in the charge/discharge rate led to an incomplete return of the specific capacity, which indicates their partial degradation during accelerated charging.

Conclusion

The paper presents the results of a study of the efficiency of using Fe_xNi_{100-x} nanotubes as anode materials for lithium-ion batteries. In the course of the experiments, it was found that an increase in the nickel concentration in the structure to 40 and 60 at.% leads to a sharp increase in the resource number of cycles by more than two times in comparison with iron nanotubes. This difference in the resource lifetime is due to the higher stability of Fe_xNi_{100-x} nanotubes with a nickel concentration of more than 40 at.% To destruction, as well as resistance to oxidation.

Acknowledgements

This study was funded by the Ministry of Education and Science of the Republic of Kazakhstan (grant AP05133578).

References

[1] K.K. Kadyrzhanov et al., Nanomaterials **9**(8) (2019) 1079.
[2] Ye. Wu et al., Nature **430**(6995) (2004) 61.
[3] M. Hayashi et al., Physical review letters **97** (2006) 207205.
[4] Lv. Ruitao et al., Catalysts **9**(2) (2019) 152.
[5] A.V. Krasheninnikov et al., Physical Review B **63**(24) (2001) 245405.
[6] Zhou et al., Nano-Micro Letters **11**(1) (2019) 40.
[7] E. Katz, Magnetochemistry **5**(4) (2019) 61.
[8] C. Liang et al., Energy & Environmental Science **13**(1) (2020) 86-95.
[9] K.V. Frolov et al., Journal of Magnetism and Magnetic Materials **489** (2019) 165415.
[10] M. Krajewski et al., Materials Chemistry and Physics **246** (2020) 122812.
[11] A.E. Shumskaya et al., Journal of Alloys and Compounds **810** (2019) 151874.
[12] A.-M. Bialostocka et al., Scientific reports **10**(1) (2020) 1-8.
[13] M.H. Abbas et al., Journal of Applied Physics **125**(17) (2019) 173902.
[14] A.E. Shumskaya et al., Journal of Alloys and Compounds **810** (2019) 151874.
[15] A.E. Shumskaya et al., Progress In Electromagnetics Research **75** (2017) 23-30.
[16] A.L. Kozlovskiy et al., Progress In Electromagnetics Research **82** (2019) 157-166.

[17] M.V. Zdorovets, A.L. Kozlovskiy, Journal of Alloys and Compounds **815** (2020) 152450.
[18] A. Kozlovskiy et al., Materials Research Express **6**(8) (2019) 085074.
[19] M. Fadeev et al., Colloids and Surfaces A: Physicochemical and Engineering Aspects **603** (2020) 125178.
[20] Zhao Zhi-Wei et al., ACS applied materials & interfaces **9**(4) (2017) 3757-3765.
[21] Liu Xinxin et al., Electrochimica Acta **231** (2017) 27-35.